

# Signatures of many-body localisation in the dynamics of two-sites entanglement

Fernando Iemini,<sup>1</sup> Angelo Russomanno,<sup>1,2</sup> Davide Rossini,<sup>2</sup> Antonello Scardicchio,<sup>1,3</sup> and Rosario Fazio<sup>1,2</sup>

<sup>1</sup>*Abdus Salam ICTP, Strada Costiera 11, I-34151 Trieste, Italy*

<sup>2</sup>*NEST, Scuola Normale Superiore & Istituto Nanoscienze-CNR, I-56126 Pisa, Italy*

<sup>3</sup>*INFN, Sezione di Trieste, Via Valerio 2, I-34127 Trieste, Italy*

(Dated: 4th September 2022)

We are able to detect clear signatures of dephasing – a distinct trait of Many-Body Localisation (MBL) – via the dynamics of two-sites entanglement, quantified through the concurrence. Using the protocol implemented in [Science **349**, 842 (2015)] we show that – in the MBL phase – the average two-site entanglement decays in time as a power law, while in the Anderson localised phase it tends to a plateau. The exponent of the power law is not universal and shows a clear dependence on the strength of the interaction. This behaviour is also qualitatively different in the ergodic phase where the two-site entanglement decays exponentially. All the results are obtained by means of time-dependent density matrix renormalisation group simulations; they are corroborated by analytical calculations on an effective model. Two-site entanglement has been already measured in cold atoms: Our analysis paves the way for the first direct experimental test of many-body dephasing in the MBL phase.

## I. INTRODUCTION

The phenomenon of many-body localisation<sup>1–3</sup> (MBL) refers to the breakdown of ergodicity in generic, disordered many-body systems due to quantum effects. This is a striking counterexample to the fundamental assumptions of statistical mechanics about the thermalization of an isolated system. For any non-integrable, classical many-body Hamiltonian system, the dynamics is ergodic in phase space leading eventually to thermalization. In classical mechanics this occurs even for systems close to integrability via Arnold diffusion, a phenomenon strictly related to the celebrated KAM theorem<sup>4,5</sup>. In quantum systems there is a striking exception: destructive interference between matter waves forbids a system in the MBL phase to thermalize. Quantum effects make the system non-ergodic: no part of it acts as reservoir for the rest of the system.

The existence of MBL is astonishing at first sight: Due to presence of interactions one expects the quantum system to be non-integrable and to show ergodicity and thermalization<sup>6</sup>. This behaviour is however strange only apparently: it has been shown that a system in the MBL phase can be mapped to an integrable system with an extensive number of local integrals of motion<sup>7–10</sup>. Traditionally, integrable systems are isolated points in the space of Hamiltonians, both from a classical<sup>4</sup> and a quantum<sup>11</sup> perspective; in MBL, on the opposite, integrability and non-ergodicity properties do not require any fine tuning. Remarkably, MBL has been recently conjectured even in systems without disorder<sup>12,13</sup>: the contrast with the behaviour of classical systems is even more striking.

In some sense, the MBL phase is the continuation of the Anderson localised (AL) phase<sup>14,15</sup> of non-interacting particles when interaction is turned on: the two phases share several properties, mainly the absence of transport of any physical quantity. At the same time MBL has distinct features that make it qualitatively different from

Anderson localisation. From one side, while transport is frozen, correlations can still propagate in the MBL phase. This gives rise to a non-trivial dynamics of entanglement which is absent in the AL phase and which we will better discuss later. From the other, the transition to the MBL phase does not emerge in thermodynamic quantities, but rather in transport and time-correlation functions. It is a *dynamical* transition and therefore we need appropriate observables to identify it. These very special properties have been recognised thanks to a constantly growing theoretical activity whose aims are elucidating the distinguishing features of MBL and finding the ways to detect them in experiments.

Several works have characterised the MBL phase by absence of transport of charge, spin or mass<sup>1,16–18</sup> or energy<sup>19</sup>; emergent, robust integrability<sup>7,8,10,20,21</sup>; logarithmically slow but unbounded growth of entanglement<sup>22–24</sup>; a peculiarly sparse structure of eigenfunctions<sup>25,26</sup>; the behaviour of observables after a quantum quench<sup>27,28</sup>; the persistence of area law for entanglement to arbitrary temperatures and for eigenstates of arbitrary energy in the spectrum<sup>3,29–31</sup>, and the ability to protect discrete symmetries<sup>32</sup> even at infinite temperature. A comprehensive description of this activity can be found in the reviews<sup>3,33</sup>.

At the same time several different proposals were put forward in order to experimentally detect MBL. The interferometric probe based on coherent spin manipulations<sup>34</sup>, the search for revivals of the magnetization<sup>35</sup> or the temporal fluctuations around stationary values of local observables<sup>28</sup> are some of the examples.

The intense theoretical efforts of the last decade stimulated an exciting race towards its experimental verification. Last year the first beautiful experiments providing evidence of MBL appeared in cold atomic systems<sup>36,37</sup> and trapped ions<sup>38</sup>. However, it is still debatable if unique features of MBL which are not present in AL systems have been observed: experiments have focused on propagation of particles which are frozen in both phases.

It would be highly desirable to have a direct experimental test discriminating between these two cases and to have a direct probe of the dephasing mechanism of the MBL phase. From a theoretical perspective, several different observables/protocols have been proposed to this aim (see above), but, in many cases, they are difficult to implement experimentally. Purpose of this paper is to overcome these difficulties: we analyse in detail a probe of MBL which is able to discriminate it from the AL phase and is experimentally accessible, within the existing technology. In the rest of the paper we are going to show that this probe is the two-site entanglement.

The dynamics of two-site entanglement was recently measured in optical lattices and in trapped ions respectively in<sup>39</sup> and<sup>40</sup>. In the experiment of Fukuhara *et al.*<sup>39</sup>, a system of atoms governed by a Bose-Hubbard Hamiltonian was considered. The spins of the atoms are initially in a ferromagnetic phase: after flipping a spin at a given site (local quench protocol), the entanglement between neighbouring spins is measured as a function of time.

As we are going to discuss in detail, we consider a slight modification of this quench protocol, the one implemented in<sup>36</sup>. Using this protocol, and measuring both imbalance and two-site entanglement, we will be able to extract the key properties of MBL phase. In particular, we will be able to find clear differences of the MBL phase and the AL phase in the measure of the two-site entanglement.

Entanglement plays an important role in MBL. While transport (of energy, spin, mass or other macroscopically conserved quantities) is frozen both in the MBL and AL cases, quantum correlations can still propagate in the MBL phase, giving rise to entanglement between distant sites of the system. In this context, the mapping of any MBL system to an integrable system with an extensive number of local integrals of motion is crucial. Thanks to this mapping, even in absence of transport, when the *populations* in every site are stationary, it can be shown that the *coherences* of distant sites evolve in a non-trivial way (more details are in Section V). This phenomenon is defined as many-body dephasing: it is the ultimate responsible for an unbounded (but slow) growth of the entanglement entropy. The situation in the AL phase is very different. In this case, the propagation of correlations and the entanglement growth stop after a while: entanglement properties give indeed a clear signature of MBL.

Several studies (see e.g.<sup>22–24,41,42</sup>) show the evolution of the entanglement entropy of large blocks in disordered spin chains. The logarithmic growth of the entropy<sup>22–24</sup>, intimately related to the existence of an extensive number of local integrals of motions, has been identified as a unique trait of MBL. However, despite recent very interesting progresses<sup>43</sup>, block entanglement entropy is very hard to be measured in a many-body context (virtually impossible on increasing the size of the block). On the opposite, the two-site entanglement we are considering is directly accessible in a cold-atoms experiment.

The paper is organised as follows. In the next section we will introduce the model and the quench protocol we are going to simulate. Both are chosen to be essentially identical to those implemented in the experiment<sup>36</sup>. The two-site entanglement will be quantified through the concurrence defined in Section III. Section IV contains the results of our density matrix renormalisation group simulations. They show that the MBL phase is characterised by a typical power-law decay of the concurrence. This behaviour strongly contrasts with AL where the concurrence reaches a non-vanishing stationary value; it is also very different from the ergodic phase, where the concurrence abruptly vanishes after a short transient. We are able to study how the AL phase is reached as a vanishing-interaction limit of the MBL: The power-law decay of the concurrence starts after a stationary, metastable, plateau whose extension in time diverges as a power law when the interaction vanishes. In Section V, we will show that the power-law decay of the concurrence is reproduced by a phenomenological integrable model of interacting qubits (the so-called “ $\ell$ -bit model”): This is in agreement with the fact that our MBL system can be mapped over an integrable system. In Section VI, we will discuss a number of additional effects (the role of number fluctuations, finite temperature, control of laser pulses) that may arise when extracting the entanglement from experimental data. In the same Section we will show that a (more easily measurable) bound to the concurrence exists: it gives very accurate results and faithfully reproduces the essential phenomenology. Finally, Section VII is devoted to our conclusions and perspectives of future work.

## II. THE MODEL

The model we consider is a generalisation of the Aubry-André model<sup>44</sup>. It can be realised in a two-species Bose-Hubbard model in the presence of a periodic potential incommensurate with the lattice spacing. This kind of potential is also defined as quasi-periodic, pseudo-random or Aubry-André potential. In the limit in which the on-site interaction is dominant with respect to the hopping, fluctuations in the number of particles in each site are frozen. It is then possible to derive an effective Hamiltonian in the sub-space in which the occupation is one particle per site. Here the dynamics is governed by an spin-1/2  $XXZ$  Hamiltonian<sup>45,46</sup> where the two eigenstates of  $\hat{S}_i^z$  represent the occupation of the  $i$ -th site by one of the two species. In the presence of Aubry-André potential the effective spin model includes also an inhomogeneous magnetic field leading to the Hamiltonian

$$\hat{H} = - \sum_i \left[ J(\hat{S}_i^+ \hat{S}_{i+1}^- + H.c.) + V \hat{S}_i^z \hat{S}_{i+1}^z \right] + \Delta \sum_i \cos(2\pi\beta i + \phi) \hat{S}_i^z, \quad (1)$$

with  $\hat{S}_i^{+(-)}$  the raising (lowering) operators. We will consider a one-dimensional optical lattice with  $L$  sites. The third term in the Hamiltonian in Eq. (1) is due to the external quasi-periodic on-site potential: The coupling strength appears as the parameter  $\Delta$ , the inverse of the incommensurate wavelength as the irrational number  $\beta$  and  $\phi$  is a phase.

Eq.(1) can be mapped, via a Jordan-Wigner transformation, onto a spinless fermionic Hubbard model with an Aubry-André onsite chemical potential.

$$\hat{H} = - \sum_i \left[ J (a_j^\dagger a_{i+1} + H.c.) + V \hat{n}_i \hat{n}_{i+1} \right] + \Delta \cos(2\pi\beta i + \phi) \hat{n}_i, \quad (2)$$

where  $a_i^{(\dagger)}$  is the creation (annihilation) fermion operator,  $\hat{n}_i = a_i^\dagger a_i$  the local number operator,  $J$  the tunneling matrix element between neighbouring sites, and  $V$  the nearest-neighbour interaction. The external potential appears as a quasi-periodic chemical potential of amplitude  $\Delta$ . The existence of a MBL phase in this model was rigorously established in Ref. [47]

In the non-interacting case ( $V = 0$ ), when the amplitude  $\Delta$  of the quasi-periodic potential overcomes a threshold  $\Delta_c = 2$ , the system undergoes a transition from an ergodic to an AL phase<sup>44</sup>. This transition has been recently observed in an experiment on cold atoms<sup>48</sup>.

The interacting case ( $V \neq 0$ ) presents three distinct phases, depending on the choice of the coupling constants: ergodic, MBL and AL phases. Although an accurate analysis of the phase diagram is not the aim of this work, we need to identify the parameters leading to the different phases. To this aim we have performed an analysis of the different phases, without however dwelling on the precise location of the phase boundaries. The resulting (approximate) phase diagram in the  $\Delta - V$  plane is reported in Appendix A.

In order to detect signatures of the MBL in the two-site entanglement, we will study its time-dependence after a quantum quench. The protocol we consider is the same as in Ref. [36]. We start initialising the system in the Néel state

$$|\psi(t=0)\rangle = |\uparrow, \downarrow, \dots, \uparrow, \downarrow\rangle. \quad (3)$$

Then, we follow its time evolution governed by the Hamiltonian Eq. (1) (therefore we will work in the subspace with total conserved spin  $S_z = 0$ ). We average the quantities of interest over many realisations of pseudo-disorder, through a random sampling of the phase  $\phi$  in the on-site pseudo-random potential. Through the rest of the paper, we will fix the inverse wavelength of the quasi-random potential as  $\beta = 532/738$ . We make this choice because this is the better approximation to an irrational number which can be done in the experiments (it is the one used in Ref. [36]). We further set  $J = 1$  and  $\hbar = 1$ .

### III. TWO-SITE ENTANGLEMENT AND THE CONCURRENCE

In the model defined in Eq.(1), the entanglement between two-sites can be quantified through the concurrence<sup>49</sup>.

We start our analysis defining the concurrence between two sites in a system of interacting spin-1/2, like the one in Eq. (1). We consider two sites of the system,  $i$  and  $j$ , and we define  $\rho_{i,j}$  as the reduced density matrix describing the subsystem formed by these two sites. We remind the reader that the concurrence  $C_{i,j}$  of two spins is a measure of the entanglement of the two spins minimised over all the possible decompositions of the matrix

$$\rho_{i,j} = \sum_{a=1,\dots,4} p_a |\psi_a\rangle \langle \psi_a|, \quad (4)$$

with arbitrary states  $\psi_a$  and  $p_a \geq 0$ .

For two spins, with this definition, the concurrence between  $i$  and  $j$  can be shown to be  $C_{i,j} = \max\{0, \lambda_{i,j}^{(1)} - \lambda_{i,j}^{(2)} - \lambda_{i,j}^{(3)} - \lambda_{i,j}^{(4)}\}$ , where  $\lambda_{i,j}^{(\alpha)}$  are the square roots of the eigenvalues of the product matrix  $R = \rho_{i,j} \tilde{\rho}_{i,j}$ , taken in descending order. The spin flipped matrix  $\tilde{\rho}$  is defined as  $\tilde{\rho} \doteq \sigma^y \otimes \sigma^y \rho^* \sigma^y \otimes \sigma^y$  (where  $\vec{\sigma}$  are the Pauli operators). If  $C_{i,j} = 0$  it means that there is a decomposition of the reduced density matrix  $\rho_{i,j}$  in which all the states  $|\psi_a\rangle$  are separable.

The concurrence has been employed several times to analyse many-body systems (see [50] for a review). Here we are going to show that its dynamics is able to distinguish between the ergodic, the MBL and the AL phases.

In the case we are considering, the  $z$  component  $S_z$  of the total spin is conserved: if we express the reduced density matrix for sites  $i, j$  in the  $z$ -basis, we find a particularly simple block-diagonal form

$$\rho_{i,j} = \begin{pmatrix} P_{\uparrow\uparrow} & 0 & 0 & 0 \\ 0 & P_{\uparrow\downarrow} & \rho_{\uparrow\downarrow} & 0 \\ 0 & \rho_{\uparrow\downarrow}^* & P_{\downarrow\uparrow} & 0 \\ 0 & 0 & 0 & P_{\downarrow\downarrow} \end{pmatrix} \quad (5)$$

where

$$\begin{aligned} P_{\uparrow\uparrow} &= \langle (\frac{1}{2} + \hat{S}_i^z)(\frac{1}{2} + \hat{S}_j^z) \rangle \\ P_{\uparrow\downarrow} &= \langle (\frac{1}{2} + \hat{S}_i^z)(\frac{1}{2} - \hat{S}_j^z) \rangle \\ P_{\downarrow\uparrow} &= \langle (\frac{1}{2} - \hat{S}_i^z)(\frac{1}{2} + \hat{S}_j^z) \rangle \\ P_{\downarrow\downarrow} &= \langle (\frac{1}{2} - \hat{S}_i^z)(\frac{1}{2} - \hat{S}_j^z) \rangle \\ \rho_{\uparrow\downarrow} &= \langle S_i^x S_j^x + S_i^y S_j^y + i[S_i^z S_j^x - S_j^z S_i^y] \rangle \end{aligned}$$

(analogous expressions can be also written in the fermionic representation). The concurrence can be analytically computed in this case

$$C_{i,j} = 2 \max \left[ 0, |\rho_{\uparrow\downarrow}| - \sqrt{P_{\uparrow\uparrow} P_{\downarrow\downarrow}} \right]. \quad (6)$$

We can see that the concurrence has been reduced to a very simple form which only contains  $zz$  expectation values and a term  $|\rho_{\uparrow\downarrow}|$  which is proportional to the local spin current (and vanishes in the long-time limit, due to localisation). It is important to keep in mind this observation in view of the analysis that will be presented in Section VI of this paper.

Because of the incommensurate potential, the concurrence (as well as other observables) will be site-dependent. To overcome this difficulty, we choose to analyse a single expression containing information on all the pairs of sites: it is the quasi-disorder average of the square concurrence summed over the sites.

$$\mathcal{C}(t) = \sum_{i,j \in \text{bulk}} \overline{C_{i,j}(t)}^2. \quad (7)$$

The bar indicates the quasi-disorder average which is performed over different realisations of  $\phi$ ; in order to avoid finite-size effects from the edges, we restrict to the bulk the sum over  $i, j$ . Precisely, we consider  $L/3 \leq i, j \leq 2L/3$ . The quantity we have defined allows to discuss in a compact way the results for the two-site entanglement. Moreover (together with the 1-tangle) it allows to extract some information on the residual multi-partite entanglement of the two selected sites<sup>51,52</sup>. The behaviour of this quantity reflects also the so-called monogamy properties of entanglement: A given spin cannot be highly entangled with more than one other spin in the system. We will see that monogamy is useful to understand the results of this paper. For simplicity, in the rest of the presentation we will refer to the quantity  $\mathcal{C}(t)$  in Eq.(7) as the concurrence.

The two-site entanglement is contained in the reduced two-site density matrix, and consequently can be expressed through the different spin-spin correlations (see Eqs.(6)). The temporal fluctuations around the stationary values of local, as well as two-spin observables, were shown to decay as power laws<sup>28</sup>. Despite providing a good insight about the dynamics, a direct relation between the behaviour of the fluctuations and the concurrence cannot be drawn because the entanglement results in a complicate function of the correlators. In general it has been shown that in most case the two-site entanglement is not directly related to the properties of correlation functions<sup>50</sup>.

Complementary to the entanglement analysis, we also study the time evolution of the imbalance in the occupation between even (e) and odd (o) sites<sup>36</sup>. In the particle representation, this is the difference in the occupation of even and odd sites  $\mathcal{I} = (N_e - N_o)/(N_e + N_o)$ ; in the spin representation it is defined as

$$\mathcal{I} = \frac{\langle S_e^z \rangle - \langle S_o^z \rangle}{1 + \langle S_e^z \rangle + \langle S_o^z \rangle}.$$

The imbalance has been measured experimentally<sup>36,37</sup>: it has been observed that it tends asymptotically to a non-vanishing stationary value, both in the MBL and

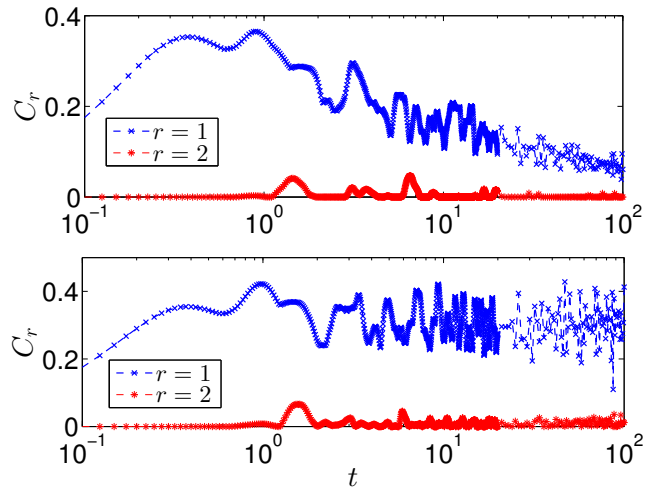


Figure 1. Evolution in time for the concurrence at distinct  $r = |i - j|$  distances, in a system with  $L = 24$  sites, averaged over 16 pseudo-disorder realisations. We consider sites at the center of the lattice, precisely,  $r = 1 \leftrightarrow (i = L/2, j = L/2 + 1)$  and  $r = 2 \leftrightarrow (i = L/2 - 1, j = L/2 + 1)$ . The top panel refers to the MBL phase, the bottom panel to the AL phase. In the ergodic phase the concurrence for  $r = 2$  is several order of magnitude smaller than  $C_{r=1}$  and could not be distinguished from zero in the scale of the plot. The results are qualitatively similar if we consider distinct sites at the bulk. The parameters are  $\Delta = 4$ ,  $V = 0$  for the bottom panel and  $\Delta = 3$ ,  $V = 1$  for the top panel.

AL phases. As we are going to show, analysing the time-dependence of the imbalance and of the concurrence, we can distinguish between the three different phases. More importantly, we can also capture the subtle dephasing mechanisms occurring in the MBL phase.

#### IV. RESULTS

This Section will be entirely devoted to the discussion of the outcomes of our simulations of the dynamics of the concurrence and the imbalance. In all the simulations discussed in this Section, we initially prepare the system in the state  $|\psi(t=0)\rangle$  (see Eq. (3)) and we study its subsequent evolution. To better compare with the existing results on the relation between many-body dephasing and growth of entanglement, we will also compare our results to the behaviour of the entropy. The message we would like to convey is that the signatures of MBL that emerge in the entanglement entropy are evident also in the two-site entanglement, but the last object has the important advantage of being easier to access in an experiment.

The dynamics of the model defined by Eq. (1) has been simulated by the time-evolving block decimation (TEBD) on matrix product states (MPS)<sup>53,54</sup>. We used a time step  $\Delta t \leq 0.1$  (depending on the model parameters), a maximum bond dimension  $m = 200$  for the MPS, and a Trotter order equal to 4, leading to negligible error



thresholds for all observables under analysis. In the specific case of non-interacting systems, however, we have evolved the state in time using the covariance matrix (to make use of the simplifications arising for quadratic Hamiltonians). We have considered systems with a number of sites  $L = 20 - 30$ : the results do not suffer of appreciable finite size corrections.

Since the definition in Eq. (7) involves a summation over many lattice points, it is useful to understand if there are dominant contributions to the sum. This analysis is shown in Fig. 1, where the concurrence is plotted as a function of time for nearest-neighbour and next-nearest-neighbour lattice sites. The coupling constants are chosen in such a way to have curves in the AL (bottom) and MBL (top) phase. We did not plot similar curves for the ergodic phase as the next to neighbour concurrence could not be distinguished from zero on the scale of the plot. In all of the phases, concurrence between sites distant more than one lattice constant is essentially negligible or vanishing. We believe that this behaviour could be indirectly linked to the properties of the eigenstates of the Hamiltonian Eq. (1), which display an exponential decay of the concurrence with distance between sites<sup>55</sup>. Therefore – although we use the definition in Eq. (7) – it is useful to keep in mind that the results we are going to present in the rest of the Section essentially reflect the behaviour of the nearest-neighbour concurrence.

In the following subsections we will discuss in detail the dynamics of our system in the AL, MBL and ergodic phases.

### A. Anderson localised phase

We first consider the case with  $V = 0$ , hence discussing the properties of the two-site entanglement in the AL phase. In the absence of interactions, the Hamiltonian reduces to a quadratic fermion model: its dynamics can be easily studied through the evaluation of the corresponding two-point correlation functions. In Fig. 2, the concurrence and the imbalance are plotted as a function of time for different disorder strengths. We only present the case  $L = 24$  to be consistent with the numerical simulations of the interacting systems: we simulated much larger lattices lengths without seeing appreciable differences. After a non-trivial transient, that we will comment later, both the concurrence and the imbalance saturate oscillating around a stationary condition that depends on the value of  $\Delta$ . A key observation is that both the concurrence and the imbalance saturate roughly at the same time: In the Anderson insulator the entanglement has no time evolution in the regime where the spin dynamics is frozen. We will see that in the MBL phase the behaviour is qualitatively different.

In analogy with the stationary value of the imbalance<sup>36</sup>, also the corresponding two-site entanglement is larger on increasing  $\Delta$  and moving deeper in the localised phase. This behaviour can be qualitatively understood

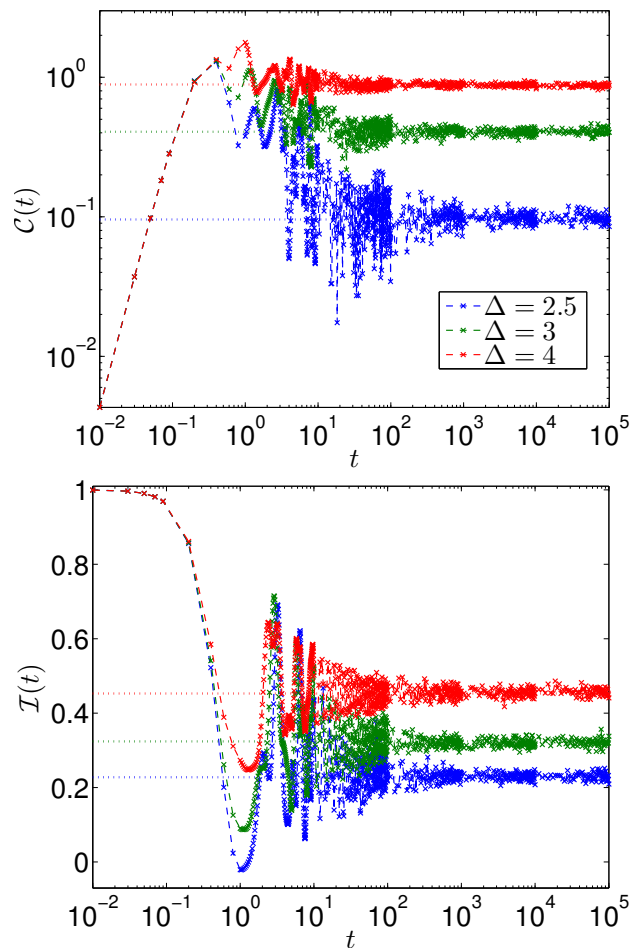


Figure 2. Time evolution for the concurrence (top) and the imbalance (bottom) in the Anderson localised phase (the values of  $\Delta$  are chosen accordingly). The system has  $L = 24$  sites and results have been averaged over  $10^2$  realisations of the pseudo-disorder. The colour code of the top and bottom panels is the same.

as follows. Starting from the factorized state Eq. (3), the short-time ( $t \lesssim 1$ ) increase of entanglement is almost independent of  $\Delta$  and it is essentially due to the exchange coupling terms (the hopping in the fermion language) in Eq. (1). Due to the many-body dynamics, the two-site entanglement starts then to decrease until a time  $t^*$ , after which its subsequent dynamics is frozen. We find that  $t^*$  decreases with  $\Delta$  (see Fig. 2-(top)): the larger is  $\Delta$ , the deeper the system is in the localised phase, the earlier the concurrence will freeze, attaining indeed a larger stationary value. The time at which the dynamics is frozen,  $t^*$  should diverge when  $\Delta \rightarrow 2$  as a power law, i.e.  $t^* \sim (\Delta - 2)^{-\nu}$ . We did not perform a detailed analysis as this aspect is tangential to the core of the work.

We have observed that, after the initial dynamics ( $t \sim 1$ ), the concurrence shows a small decay until its saturation. For later comparison with the MBL case, it is useful to have a closer look to this intermediate regime. To this aim we plot both the two-site entanglement

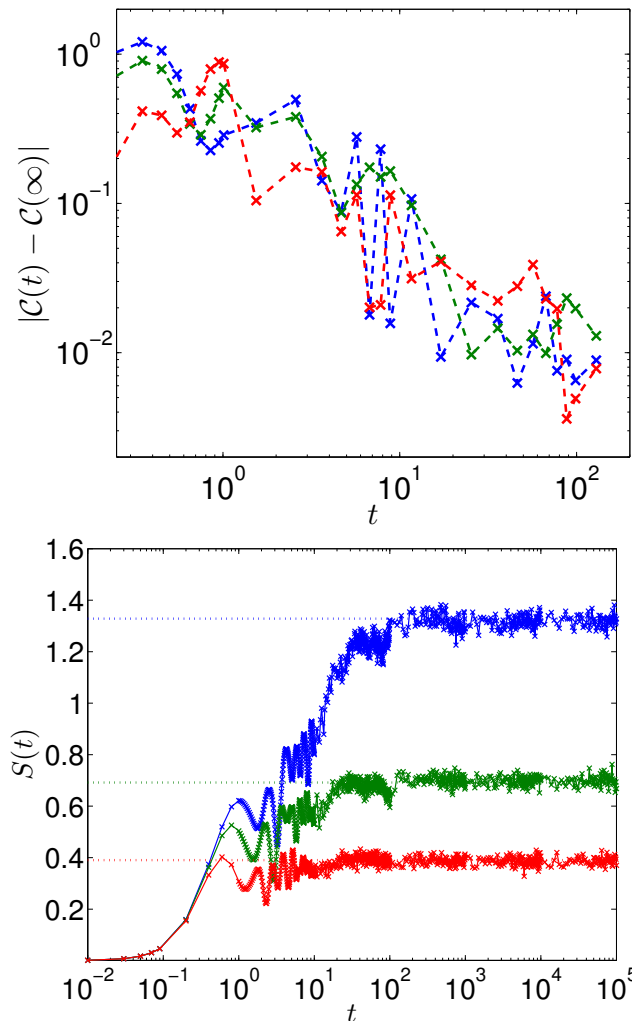


Figure 3. (Top) Decay of the concurrence to its long-time stationary value for  $t \gtrsim 1$ . In this regime the concurrence decays as a power-law with an exponent independent on  $\Delta$ . In the plot we averaged the concurrence over small time bins in order to make the decay clearer. (Bottom) For comparison, we plot the half-chain entanglement entropy in the Anderson localised phase as a function of time. In the regime in which the concurrence decays to its stationary value also the entanglement entropy and the imbalance (Fig. 2-(bottom)) evolve in time, later everything saturates to a stationary value. The numerical values and the colour code are the same as in Fig. 2.

(Fig. 2-(top)) and the block entropy (Fig. 3-(bottom)). To better analyse the decay of the concurrence, we subtract its long-time value (see Fig. 3-(top)). In this intermediate regime, both the entropy and the concurrence, as well as the imbalance, evolve with time: The system has not yet frozen. On the opposite, we will see in the MBL phase that the two-site entanglement shows a power law decay only in the long-time limit and not in an intermediate regime. Moreover, in this asymptotic regime, the spin dynamics is frozen and the MBL dephasing takes place. Therefore, the power law decay in the AL phase and the one in the MBL phase are different phenom-

ena which have to be distinguished from each other: the first one is a transient effect occurring before the entanglement and spin dynamics freeze, the second one is an asymptotic phenomenon occurring when the spin dynamics has already frozen. Another clear difference with the MBL phase emerges also in the decay of the concurrence to its long-time limit: apparently the exponent of the power law does not depend on the disorder strength (see Fig. 3-(top)); we are going to see that the power law decay in the MBL phase behaves very differently.

## B. Many-body localised phase

Equipped with the results for the AL phase, we are now going to discuss what happens in the presence of interaction. We first consider parameters for which the

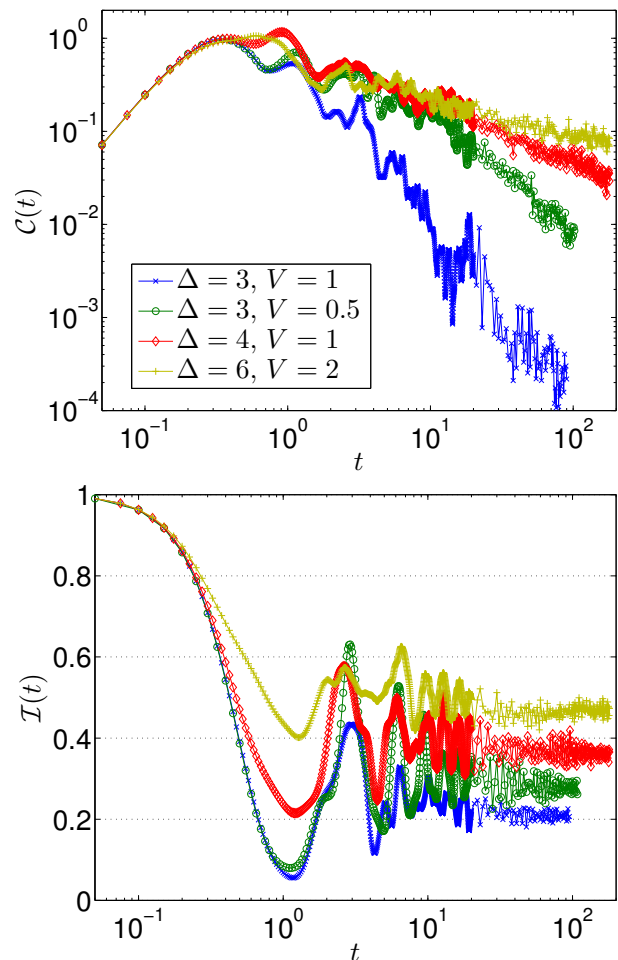


Figure 4. Time-evolution for the concurrence (top) and imbalance (bottom) in the MBL phase. The plot for the concurrence is set in log-log scale in order to highlight the power-law decay in the MBL phase. The system has  $L = 24$  sites and different strengths of the pseudo-random potential amplitude  $\Delta$  are considered. The data shown are averaged over 30 realisations of the pseudo-random potential.

system is in the MBL phase (see the phase diagram in Appendix A). As outlined in the Introduction, the spin dynamics in the MBL phase is frozen but correlations evolve in time due to a many-body dephasing phenomenon which is connected to the existence of an extensive number of local integrals of motion. This dephasing peculiarly affects the behaviour of entanglement: a signature of this phenomenon can be seen in the evolution of the half-system entanglement entropy which increases logarithmically in time only in the MBL phase. We are going to show that signatures of these effects can also be seen in the two-site entanglement which shows a very special long-time behaviour unique to the MBL phase.

In Fig. 4, we show the dynamical behaviour of the concurrence (upper panel) and the imbalance (lower panel) in the MBL phase. As discussed previously for the AL phase, also here the initial dynamics – up to  $t \lesssim 1$  – is independent of  $\Delta$  and  $V$ : in this time regime, the only relevant terms of the Hamiltonian in Eq. (1) are those containing the exchange couplings.

The interesting regime occurs for longer times,  $t \gtrsim 1$ . In a region where the imbalance has already frozen, we clearly see a power-law decay for the concurrence with an exponent that depends both on  $V$  and  $\Delta$ . This power law decay of the concurrence has to be contrasted with the saturation observed in the AL phase. We find indeed that, in the presence of interactions, there is a regime where transport is absent but still the two site entanglement evolves in time. It is important to stress that the dephasing mechanism which leads to the power law decay of the two-site entanglement is the same as the one giving rise to the logarithmic growth of the entanglement entropy. We will discuss in detail this dephasing mechanism in Section V. The important new ingredient is that two-site entanglement is “easy” to measure. The comparison of Fig. 2 and Fig. 4 shows that, while the imbalance saturates both in the AL and MBL phases, the concurrence is qualitatively different in the two cases.

The difference between AL and MBL in the concurrence can be further highlighted in the weakly interacting limit  $V \ll 1$ . In this case, discussed extensively in Appendix B, two regimes appear in the dynamics of concurrence. After the common transient, the concurrence reaches a plateau typical of the AL phase. The plateau occurs for times  $1 \leq t \leq t_{int} \sim 1/V$  (for weak interactions it is possible to separate this time scale). Only at later times,  $t \geq t_{int} \sim 1/V$ , interactions set in and the concurrence starts to decay as a power law. A detailed analysis of this regime together with the determination of  $t_{int}$  as a function of the interaction  $V$  is presented in the Appendix B

One final comment is now in order. The results we presented are for the average of the two-site entanglement; its statistics is expected to be very interesting as well. It is known from perturbative constructions of the integrals of motion<sup>8</sup> that the mechanism for delocalisation (and in general for mixing distant spins with a local spin) is to construct long non-local operators which – at

a variance with respect to the AL case – are not simply bilinear in the raising and lowering operators. Therefore the dynamics of one spin gets mixed with a line of spins of length  $\xi_{MBL}$  which is the MBL localisation length. In this way, the statistics of recurrences of concurrence (the times at which the concurrence  $C_{i,j}$  returns to be non-zero) is less regular than in the AL case: after averaging, this leads to the power law decay.

### C. Ergodic phase

We conclude the discussion of the numerical simulation by analysing the concurrence in the ergodic phase. In the cases we consider interactions are chosen to be  $V \gtrsim 1$ . In this regime numerical simulations are much harder and we are able to follow the dynamics reliably up to  $t \sim 10$ . In Fig. (5) (bottom) we show the imbalance as a function of time. In the ergodic phase it should go to zero in the long-time limit. As we can see, times  $t > 10$  are needed for a full equilibration. It is however clear from the data that the imbalance is still decaying towards its stationary value.

The behaviour of the concurrence, Fig. (5) (top), differs qualitatively from the previous cases. Here it vanishes abruptly. The data seem to indicate an exponential decay (especially clear in the absence of potential). Since its decay is too fast, it is hard to unambiguously differentiate from an exponential or a high order power-law decay (see Fig. (5)). The ergodic phase is further characterised by large revivals with a typical period of the inverse of the exchange coupling.

In the long time (stationary) limit the concurrence is expected to vanish. The system will equilibrate at an effective temperature related to energy initially injected in the system. This effective temperature is much larger than one (in units of  $J$ ) for the choice of our initial states. At this temperature any trace of thermal entanglement has already disappeared<sup>50</sup>.

The different time-dependence in the decay of two-site entanglement is intimately connected to the monogamy of entanglement. Because the much faster propagation of the excitations in the ergodic phases, entanglement will be spread faster. Consequently two-site entanglement will decay rapidly, exponentially as observed in the simulations. The spread, and related decay in the concurrence, is slower in the MBL phase.

## V. CONCURRENCE IN THE $\ell$ -BIT MODEL

In order to corroborate the results of our numerical simulation we are going to show that the phenomenology we just discussed can be obtained by an effective model expressed in terms of the local integrals of motion. Within this effective model it is possible to obtain semi-analytical results and – most importantly – it is natural to link the behaviour of the two-sites entanglement

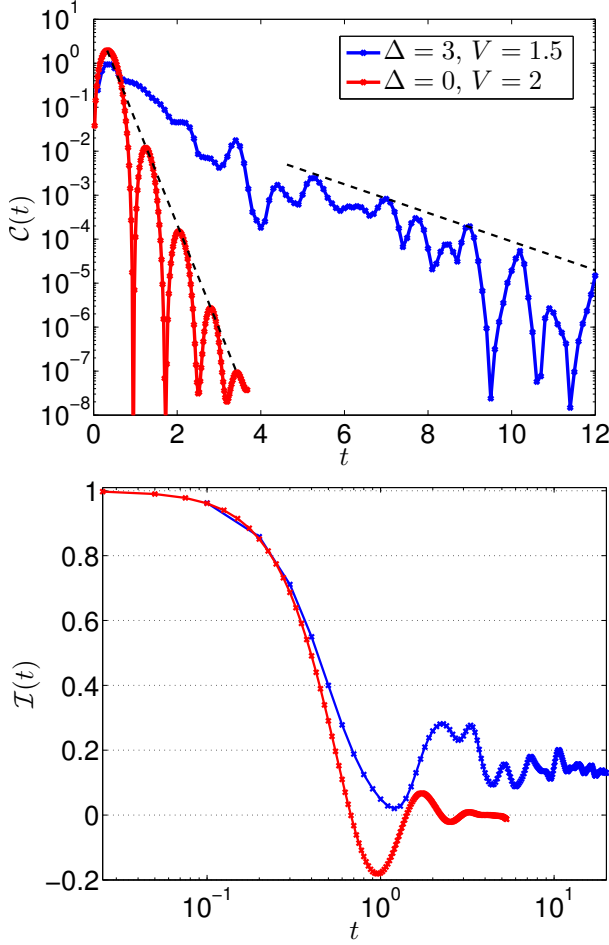


Figure 5. Time-evolution for the concurrence and the imbalance in the ergodic phase. The system has  $L = 24$  sites (for  $\Delta = 0, V = 2$  the system is slightly larger with  $L = 48$  sites) and is averaged over  $\sim 30$  realisations of the pseudo-random potential. The black lines are just a guide to the eye to indicate the exponential decay.

to the dephasing typical of the MBL phase.

As already mentioned in the Introduction, a key feature of MBL phase is that it possesses an extensive number of local integrals of motion. This notion of integrability leads to a very powerful description of the system in terms of an effective Hamiltonian: the so called phenomenological  $\ell$ -bit model<sup>3,7</sup>

$$\hat{H} = \sum_j h_j \hat{\tau}_j^z + \sum_{j \neq l} \mathcal{J}_{jl} \hat{\tau}_j^z \hat{\tau}_l^z + \dots \quad (8)$$

Here,  $\{\hat{\tau}_j^x, \hat{\tau}_j^y, \hat{\tau}_j^z\}$  are the localised spin-1/2 operators associated to the local integrals of motions (in this context, they are also called the  $\ell$ -bit operators: “ $\ell$ ” stands for localised). In the previous definition,  $h_j$  are random fields, and  $\mathcal{J}_{jl} = \mathcal{W}_{jl} e^{-\alpha|j-l|}$  are the interaction terms, with  $\mathcal{W}_{jl}$  assumed to be a random variable uniformly distributed in the range  $[-W, W]$ <sup>56</sup>. Further terms in the Hamiltonian include  $n$ -body interactions, with  $n > 2$ ,

which, for simplicity, we will not consider here and are irrelevant for our purposes (see later). The spins  $\hat{\tau}_i$  are local functions of the physical spins: the precise form of this mapping is not important for the present work. In an Anderson insulator, the couplings  $\mathcal{J}_{jl}$  are vanishing and a set of independent non-interacting spins is sufficient for an effective description of the dynamics on a distance larger than the localization length.

The analysis of the model in Eq. (8) gives us the possibility to see in a different perspective and clearly understand the difference between the AL and MBL phases in the behaviour of the two-site entanglement. From one side, the Hamiltonian of an Anderson insulator will only lead to single-bit rotations (that do not modify the entanglement). On the opposite, in the MBL phase, the second term of Eq.(8) is responsible for two-qubit gates (controlled phase-shifts) that lead to a time-dependence of the entanglement. These terms are the ones leading to the logarithmic growth of the entropy<sup>22–24</sup> (higher order contributions to the Hamiltonian do not change the picture). We are going to show that they also lead to the power-law decay of the concurrence.

The dynamics generated by the phenomenological  $\ell$ -bit model gives a meaningful comparison with the exact dynamics of the Hamiltonian of Eq. (1) for times  $t > 1$ . In this time-regime, the interactions and the quasi-periodic Aubry-André potential become relevant (in the initial transient we saw that only the exchange terms affect the concurrence dynamics).

The dynamical protocol we consider goes as follows. The system is initially prepared in a generic separable state given by

$$|\psi_o\rangle = \otimes_{j=1}^L [\cos(\phi_j) |\uparrow\rangle + e^{i\theta_j} \sin(\phi_j) |\downarrow\rangle]$$

where  $\{|\uparrow\rangle, |\downarrow\rangle\}$  are the eigenstates of the  $\hat{\tau}_j^z$  operator and  $\phi_j, \theta_j$  are randomly chosen parameters. The time evolution of the  $\ell$ -bit operators can be easily computed (see Appendix C) and the concurrence can be determined as a function of time. In our analysis, we average over distinct initial states (different realisations of  $\{\theta_j\}, \{\phi_j\}$ ), local disorder terms “ $h_j$ ” (despite it has absolutely no effect on the concurrence) and interacting terms “ $\mathcal{W}_{jl}$ ”.

As already mentioned, when we are in the AL phase, the Hamiltonian Eq. (8) induces a local dynamics: it cannot lead to any changes in the entanglement. For the MBL phase the situation is much more intriguing because of the coupling between the  $\ell$ -bit operators. In Fig 6, we plot the concurrence as a function of time. As already mentioned, we average over random realisations of the external fields, couplings and initial preparation of the state. We see that the concurrence decays as a power law, fully confirming the fact that this form of the two-site entanglement behaviour is a typical feature of MBL.



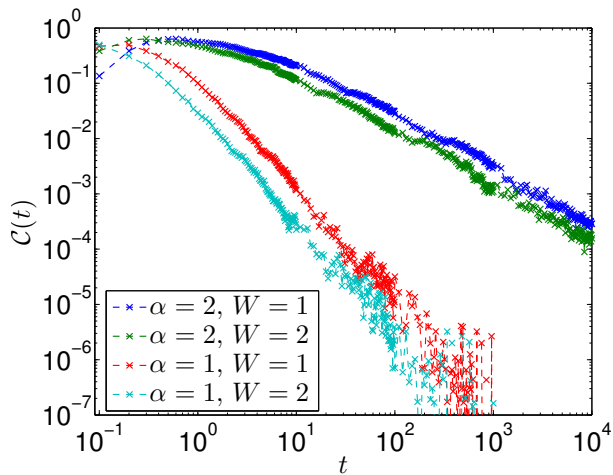


Figure 6. Time-evolution for the concurrence in the  $\ell$ -bit model (Eq. (8)). The plot is set in log-log scale to show the power-law decay. The model is taken with  $L = 72$  sites, and results are averaged over  $10^2$  simulations where the initial state as well as the couplings in the Hamiltonian (8) are chosen randomly.

## VI. EXPERIMENTAL ISSUES AND A BOUND TO THE CONCURRENCE

Experimentally, the detection of concurrence for unknown two-site reduced density matrices might face some imperfections, such as the lack of complete experimental control in the measurements, on-site number fluctuations or thermal smearing. For a better comparison with the experiments it is important to consider all these issues.

The spin-model of Eq. (1) does not include number fluctuations present in the native two-species Bose-Hubbard Hamiltonian. A detailed analysis of these effect has been performed in [57]. As long as the on-site repulsion between the bosons is much larger than their hopping (in practice a factor five in this ratio is enough) the predictions of the effective spin models are reliable. As far as thermal fluctuations are concerned, the analysis of [57] confirms that – as expected – our model is reliable for experiments if the temperature is of the order of few percents of the on-site interaction.

It is of particular importance here to address the lack of control in the pulses needed to measure the entanglement: this fact leads to the detection of smaller correlation values. In connection with this issue, we provide below a very useful lower bound for the concurrence. For the present model, the qualitative behaviour of this bound agrees with the actual concurrence dynamics with high fidelity. For longer times in the dynamics the agreement becomes even quantitative: The bound becomes tighter with increasing time.

A full two-site reduced density matrix can be obtained by measuring all of its spin-spin correlation functions. In principle, such measurements could be performed in a cold-atoms setup by first applying pulses on

each individual spin site and then allowing it to freely rotate. After the appropriate time-interval has elapsed, the measurement is performed in a fixed basis (*e.g.*, in the  $z$  eigenstate basis:  $\{|\uparrow\rangle, |\downarrow\rangle\}$ ). However, in cold atoms implementation of Hubbard models, pulses on individual spin sites are not yet implemented. In this case, only a global pulse on both spin sites is allowed, and consequently only measurements spin-spin correlations along the same direction are performed. In this case the reduced density matrix element  $\rho_{\uparrow\downarrow}$  is approximated to

$$\tilde{\rho}_{\uparrow\downarrow} = \langle S_i^x S_j^x + S_i^y S_j^y \rangle = \Re(\rho_{\uparrow\downarrow}). \quad (9)$$

Recalling the expression for the concurrence Eq. (6), since  $|\tilde{\rho}_{\uparrow\downarrow}| \leq |\rho_{\uparrow\downarrow}|$ , we obtain the lower bound

$$\tilde{C}_{ij} \equiv 2 \max \left[ 0, |\tilde{\rho}_{\uparrow\downarrow}| - \sqrt{P_{\uparrow\uparrow} P_{\downarrow\downarrow}} \right] \leq C_{ij}. \quad (10)$$

Since the concurrence is generated essentially only between nearest-neighbour sites, let us focus on this case. Here,  $\rho_{\uparrow\downarrow}$  has a particularly simple form,  $\rho_{\uparrow\downarrow} = a_i^\dagger a_{i+1}$ , and a clear physical interpretation. As we can see in Eq.(9), the bound for the concurrence does not involve the imaginary parts of the hopping terms, which physically correspond to the spin current between the neighbouring sites  $\propto \Im(a_i^\dagger a_{i+1})$ . Since in the localised phase we should asymptotically expect no current in the system (despite still having a flow of information/correlations) the above bound for the concurrence should become tighter with increasing of time. Precisely,  $\tilde{\rho}_{\uparrow\downarrow} \sim \rho_{\uparrow\downarrow}$  for  $t \gg 1$ , and consequently  $\tilde{C}_{ij} \sim C_{ij}$ .

Fig. 7 compares the dynamics of the concurrence (in colour) with its bound (grey) for the three different phases AL (panels a and b), MBL (panel c), and ergodic (panel d). It is evident that, except for the initial transient, the bound faithfully reproduces the behaviour of the two-site entanglement thus making the experimental detection easier.

## VII. CONCLUSIONS

Aim of the paper was to show that distinct features of the many-body localised phase can be detected through a measure of two-site entanglement. The time-dependence of the concurrence, the measure we used to quantify two-site entanglement, can clearly distinguish between MBL, AL and ergodic phases. In order to highlight this different behaviour we studied the dynamics of two-site entanglement in a quantum quench as experimentally implemented in the work by Schreiber *et al.*<sup>36</sup>. We stress the importance on the choice of the quantum correlation quantifier as well as in the initial state, since different choices could lead to distinct long-time behaviours<sup>65</sup>.

The system we considered is a two-species Bose-Hubbard model in an optical lattice undergoing a quasi-periodic Aubry-André potential. Ignoring number fluctuations, this model reduces to the  $XXZ$ -model, studied

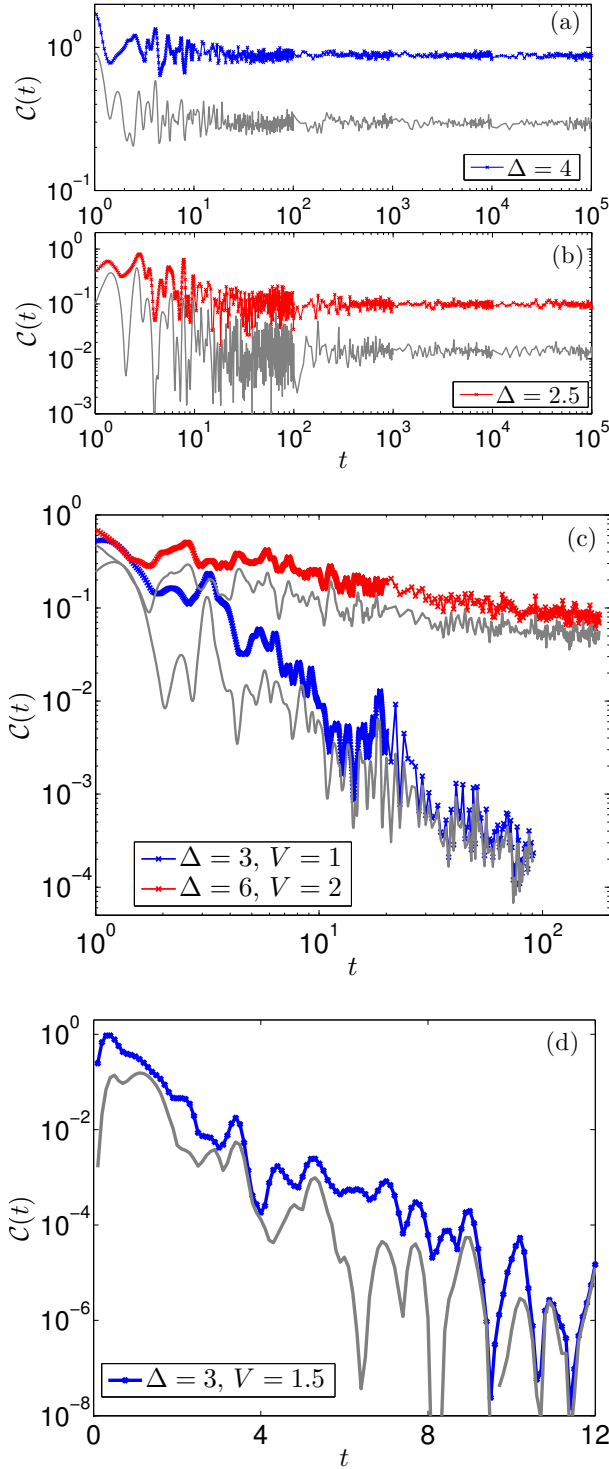


Figure 7. Experimental bound: Time-evolution for the Concurrence (colour) and its experimental bound (grey) based on measurements performed with global pulses at both sites (see main text), in the three distinct phases: AL (panels a and b), MBL (panel c), and ergodic (panel d).

here. Our results were based on time-dependent density matrix renormalisation group simulations complemented

by semi-analytical calculations on an effective model. After an initial transient, dominated by the kinetic term in the Hamiltonian, the concurrence dynamics in the different phases shows a strikingly different behaviour. The two-site entanglement saturates to a non-vanishing constant in the AL phase while it decays as a power law in the MBL phase and exponentially fast in the ergodic one.

In order to corroborate the claim that the power-law decay is a characteristic trait of the MBL phase, we analysed the same problem using an integrable phenomenological  $\ell$ -bit model<sup>3,7</sup>. This model is known to capture the essence of the MBL phase: this is a consequence of the unitary equivalence of any MBL system to an integrable one with localised integrals of motion. Exploiting the integrability of the phenomenological model, we could compute in a semi-analytical way the two-site entanglement showing the same power-law decay occurring in the MBL phase of our system.

The main advantage of our proposal relies in the fact that experimental protocols to measure the two-site concurrence have already been implemented, thus our analysis can be tested in the laboratory. In order to make a closer contact with the experiment, we also computed an useful bound to the concurrence that can be more easily measured. In the relevant time-regime this bound turns out to be very close to the actual value of the entanglement.

It is important to stress that all the results obtained in this work hold for averaged quantities. Single realisations of disorder have very different aspects and the power-law decay itself of  $C$  comes from single realisations of disorder in which  $C_{jl}$  is mostly zero except occasional “revivals.” It would be of great interest to analyse the full statistics of entanglement, something that is also experimentally accessible. In fact, it is possible that multifractal properties of the eigenstates in the MBL phase<sup>25,58,59</sup> are reflected in full counting statistics of these revivals and higher moments of  $C_{ij}$ .

A further perspective of future work will be to understand the behaviour of the power law when the transition to the ergodic phase is approached. Other interesting questions concern the behaviour of the concurrence when a local quench is performed, especially in connection with the phenomenon of the logarithmic-light-cone propagation of the correlations (see [42]).

*Note added.* After completion of this manuscript, we became aware of a related work<sup>66</sup> discussing the dynamics of two-sites quantum mutual information in the MBL phase.

## ACKNOWLEDGMENTS

We warmly thank Leonardo Mazza for useful discussions. This research was supported in part by the Italian MIUR via FIRB project RBFR12NLNA, by the EU integrated projects SIQS and QUIC and by “Progetti interni - SNS”. F. I. acknowledges financial support by

the Brazilian agencies FAPEMIG, CNPq, and INCT-IQ (National Institute of Science and Technology for Quantum Information)

### Appendix A: Phase diagram

Depending on the value of its coupling constants, the model studied in this work (Eq.(2)) presents distinct phases: Ergodic, MBL and AL phases. Although several exact results<sup>47</sup> of the general case and the phase diagram along the non-interacting line<sup>44</sup> are known, the location of the phase boundaries has not been worked out so far. A detailed analysis of the location of the phase boundaries together with their properties is beyond the scope of the present work. What we need is a reliable analysis that can tell us the coupling to choose in order to be in one of the three phases.

Therefore, our aim is an (approximate) phase diagram for the Hamiltonian in Eq.(2). We obtain it combining different approaches. More precisely, we study: (i) the time-dependence of the entanglement entropy of a block with half the system size<sup>22–24</sup>, and (ii) the level-spacing statistics of the Hamiltonian<sup>60</sup>. A detailed discussion about the way these quantities can discriminate between the different phase can be found in the cited references.

The entanglement entropy  $S_A(t)$  of a block with  $A$  sites is defined as

$$S_A = -\text{Tr}[\rho_A \log(\rho_A)], \quad (\text{A1})$$

with  $\rho_A = \text{Tr}_{\neq A}[\rho]$  the reduced state for the  $|A|$  sites. The increase in time of the entanglement entropy behaves differently in the three phases. We expect a ballistic growth with time in the ergodic phase, in contrast to a logarithmic dependence in the MBL phase and a saturation in the AL phase<sup>22–24</sup>.

We also analyse the level-spacing statistics<sup>60</sup>. The rationale behind this approach lies in the fact that the level spacing distribution is given by a Wigner-Dyson law in an ergodic system and by a Poisson law in an integrable system: as we have extensively discussed, MBL is a special case of integrable system (the reader can find more details on the spectral statistics in Refs.<sup>4,61–63</sup>). In order to distinguish the phase of the system, instead of considering the whole level-spacing statistics, we can restrict to a quantity whose average takes markedly different values on the two distributions. Having defined the gaps between adjacent many-body levels  $\{E_n\}$  as  $\delta_n = E_{n+1} - E_n \geq 0$ , we define the ratio

$$0 \leq r_n = \min\{\delta_n, \delta_{n+1}\} / \max\{\delta_n, \delta_{n+1}\} \leq 1. \quad (\text{A2})$$

We define the average of this ratio over the level spacing distribution ( $\langle r_n \rangle$ ) as the average level statistics: the different phases are characterised by a different value of this object. From the results of Ref.<sup>60</sup>, we expect to have  $\langle r_n \rangle \simeq 0.386$  in the localised phase (Poisson distribution of the level spacings), and  $\langle r_n \rangle \simeq 0.5295$  in the ergodic phase (Wigner-Dyson distribution of the level spacings).

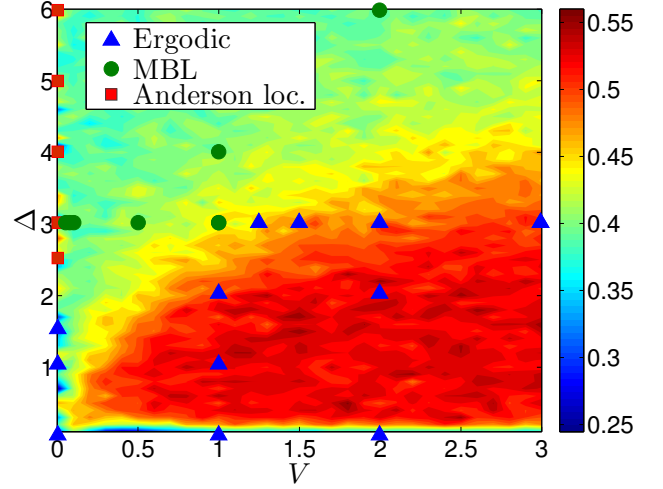


Figure 8. Phase diagram for the fermionic model (Eq. (2)) at half filling (corresponding to spin model Eq. (1) at total spin  $S_z = 0$ ). Marked points in the figure were studied using TEBD simulations, for systems up to  $L = 24$  sites, where it was analysed the half-system entanglement entropy dynamics. The colour filling corresponds to the average level statistics ( $\langle r_n \rangle$  – see the main text for a definition) for a system with  $L = 12$  sites. Only in correspondence to the marked points we can reliably say that the system is in one of the three different phases.

The colour code in Fig. 8 shows how the analysis of the level statistics discriminates between the ergodic and the localised phase. In addition, in the points of the phase diagram marked by a symbol, we have also studied the phase of the system by means of the time-dependence of the entanglement entropy. Our analysis is too simplified to draw the phase boundary (it is not important for the present paper). We are however able to discriminate the three different phases in the selected points of the phase diagram indicated by the symbols in Fig. 8. These values of the couplings will be used for the analysis of the two-site entanglement.

### Appendix B: Weak interaction limit

In the regime in which the interaction  $V$  in Eq. (1) is finite but small, typically of the order of  $10^{-2} - 10^{-1}$  in our system, we can clearly separate two different time scale. At the first one ( $t^*$ , introduced in Section IV), the two-site entanglement saturates to a plateau like in the AL phase. After the second one (which we define  $t_{int}$ ), the power-law decay typical of the MBL phase begins. In this way we can set a clear distinction between the AL and MBL regimes in the same time trace. We expect the effect of MBL dynamics to appear at times of the order of  $t_{int} \sim 1/V$ ; for small interactions this scale can be much larger than the typical time scale associated to saturation in the AL phase:  $t_{int} \gg t^*$ .

Our expectations are confirmed by the results shown

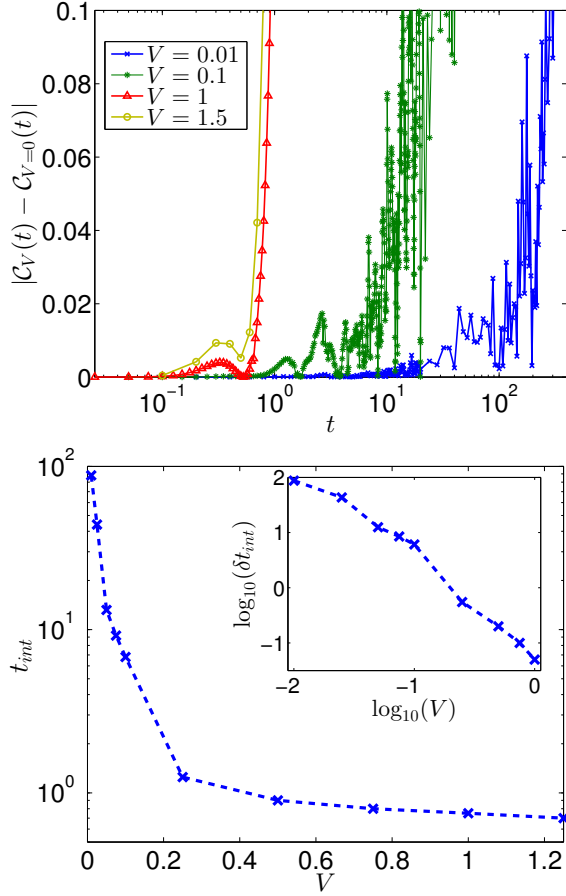


Figure 9. (top panel) the difference  $|C(t, V \neq 0) - C(t, V = 0)|$  is plotted as a function of time. The system has  $L = 24$  sites, fixed disorder strength  $\Delta = 3$ , and results are averaged over  $\sim 30$  disorder realisations. The difference remains zero up to a characteristic time  $t_{int}$  when interactions become relevant. From the analysis of the uprise of the curves it is possible to extract this characteristic time  $t_{int}$ . (bottom panel)  $t_{int}$  as a function of  $V$ . In order to extract the exponent of the power law fit, in the inset figure of the bottom panel, we plotted  $\delta t_{int} = t_{int}(V, \Delta) - t_{int}(V \gg 1, \Delta)$ , where  $t_{int}(V \gg 1, \Delta) \sim 0.7$ .

in Fig. 9. As we can see in the upper panel of the figure for very small values of  $V$ , the concurrence presents a “plateau” after the initial dynamics, where it is indistinguishable from the non-interacting case. Only after some finite time –  $t_{int}$  – the effects of interactions play a relevant role in the dynamics and the concurrence starts to decay. The two regimes are clearly visible in Fig. 9 (top). Because it is strictly related to the effect of interactions, we term  $t_{int}$  as the interaction time.

We can give an estimate of  $t_{int}$  extracting it from the time traces of the concurrence. In order to do that, we start giving a more quantitative definition of  $t_{int}$ . To this end it is illuminating to plot, at fixed disorder, the difference  $|C_V(t) - C_{V=0}(t)|$ . This is shown in Fig. 9 (top panel). As it is evident from the plots the difference remains zero up to a characteristic time  $t_{int}$  when

interactions become relevant. Fixing the pseudo-disorder strength  $\Delta$  (see Eq. (1)), the interaction time  $t_{int}$  is defined as the time at which the concurrence with  $V > 0$  starts to differ from the non-interacting one ( $V = 0$ ) more than some threshold  $\epsilon$ . We choose  $\epsilon$  in order to capture the effect of the interactions, and not just small oscillations around the non interacting dynamics. Precisely, we choose  $\epsilon = 0.025$ , the results however are qualitatively similar for slightly different values of the threshold.

The result of this analysis is reported in Fig. 9 (bottom). For the case shown in the figure, with disorder strength  $\Delta = 3$ , such interaction time corresponds to  $t_{int}(V) \propto V^{-a} + b$ , with  $a \approx 1.6$  and  $b = 0.7$  (see inset in Fig. 9 (bottom)). So we see that our expectation of a  $t_{int}$  diverging as a power law for  $V \rightarrow 0$  is confirmed, but the exponent of the power law is different from what we expected.

### Appendix C: Correlations in the $\ell$ -bit model

This appendix summarises the derivation of the time dependent spin-spin correlation functions in the effective  $\ell$ -bit model (Eq. (8)): these correlations are necessary to determine the two-spin reduced density matrix and then the two-site entanglement (see also [28]). According to the  $\ell$ -bit phenomenological model, the physical spin operators  $\{\hat{S}_j^\alpha\}_{j=1, \dots, L}^{\alpha=\mathbb{I}, x, y, z}$  of the Hamiltonian Eq. (1) are, in principle, “locally” related to the  $\ell$ -bit operators  $\{\hat{\tau}_m^\alpha\}_{m=1, \dots, L}^{\alpha=\mathbb{I}, x, y, z}$  as

$$\hat{S}_j^\alpha = \sum_n \sum_{\alpha'} \Delta_{j,n}^{\alpha, \alpha'} \hat{\tau}_n^{\alpha'} \quad (\text{C1})$$

where  $\Delta_{j,n}^{\alpha, \alpha'}$  is localised, that’s to say non-vanishing only in a finite range around  $m$ . The precise form of  $\Delta_{j,n}^{\alpha, \alpha'}$  is in general non-trivial to obtain but this is not important for us. The main message is that the  $\Delta_{j,n}^{\alpha, \alpha'}$  are localised: we expect that the properties of the  $\ell$ -bit operators and those of the physical spins are similar. This expectation is confirmed by the results shown in Section V: the concurrence obtained from the correlations of the  $\ell$ -bit operators shows the same polynomial decay as the one numerically computed for the physical spins in Section IV. In this appendix we will discuss in detail the computation of the concurrence dynamics of pairs of  $\ell$ -bit sites we have considered in Section V.

For such task we must first compute the reduced density operator for the  $m$  and  $n$  ( $\hat{\rho}_{mn}(t)$ ), which can be obtained from the correlations of its  $\ell$ -bit operators

$$\hat{\rho}_{mn}(t) = \sum_{\alpha, \alpha' = \mathbb{I}, x, y, z} \langle \hat{\tau}_m^\alpha(t) \hat{\tau}_n^{\alpha'}(t) \rangle \hat{\tau}_m^\alpha(0) \hat{\tau}_n^{\alpha'}(0). \quad (\text{C2})$$

We consider general initial uncorrelated states

$$\begin{aligned} |\psi(0)\rangle &= \otimes_{m=1}^L |\chi_m(\phi_m, \theta_m)\rangle \\ |\chi_m(\phi_m, \theta_m)\rangle &= \cos(\phi_m) |\uparrow\rangle + e^{i\theta_m} \sin(\phi_m) |\downarrow\rangle, \end{aligned}$$



where  $\{|\uparrow\rangle, |\downarrow\rangle\}$  are the eigenstates of the  $\hat{\tau}_m^z$  operator. In this way any correlated  $\ell$ -bit operators can be handled more easily, since

$$\langle \hat{\tau}_m^\alpha \hat{\tau}_n^{\alpha'} \rangle = \langle \hat{\tau}_m^\alpha \rangle \langle \hat{\tau}_n^{\alpha'} \rangle \quad (\text{C3})$$

due to the separability of the initial state, and analytically computed, as we will show below.

Since all operators in the  $\ell$ -bit model commute, it is possible to analytically compute the time evolution of any operator in the Heisenberg picture. Because we will extensively use them in our analysis, let us just briefly recall the commutation relation between the Pauli matrices

$$[\hat{\tau}_j^\alpha, \hat{\tau}_j^{\alpha'}] = 2i\epsilon_{\alpha\alpha'\beta} \hat{\tau}_j^\beta,$$

with  $\epsilon_{\alpha\alpha'\beta}$  the Levi-Civita coefficient. The  $\ell$ -bit operators evolve in the Heisenberg picture as

$$\frac{d}{dt} \hat{\tau}_m^\alpha = \frac{i}{\hbar} [\hat{H}, \hat{\tau}_m^\alpha].$$

The operators  $\hat{\tau}_m^z$  commute with the Hamiltonian  $\hat{H}$  (shown in Eq. (8)), thus they are time independent. Let us focus on the  $\alpha \neq z$  cases. Applying the commutation relations in the Heisenberg equations, we obtain

$$\dot{\hat{\tau}}_m^\alpha = \hat{\tau}_m^{\bar{\alpha}} \epsilon_{z\alpha\bar{\alpha}} \hat{A}_m \quad (\text{C4})$$

with  $\bar{\alpha} = y(x)$  for  $\alpha = x(y)$ , and

$$\hat{A}_m = -\frac{2}{\hbar} \left( h_m \mathbb{I} + 2 \sum_{j \neq m} \mathcal{J}_{mj} \hat{\tau}_j^z \right).$$

As for the  $zx$  terms we obtain

$$\langle \hat{\tau}_m^z(t) \hat{\tau}_n^x(t) \rangle = \left( e^{2i\mathcal{J}_{nm}\bar{t}} \cos^2(\phi_m) - e^{-2i\mathcal{J}_{nm}\bar{t}} \sin^2(\phi_m) \right) e^{-i\theta_n} \sin(\phi_n) \cos(\phi_n) e^{ih_n\bar{t}} K_{\bar{t}}(m, n) + H.c., \quad (\text{C8})$$

where we used that

$$\langle \hat{\tau}_m^z e^{2i\mathcal{J}_{nm}\hat{\tau}_m^z\bar{t}} \rangle = \left( e^{2i\mathcal{J}_{nm}\bar{t}} \cos^2(\phi_m) - e^{-2i\mathcal{J}_{nm}\bar{t}} \sin^2(\phi_m) \right).$$

For the  $zy$  terms we have

$$\langle \hat{\tau}_m^z(t) \hat{\tau}_n^y(t) \rangle = \left( e^{2i\mathcal{J}_{nm}\bar{t}} \cos^2(\phi_m) - e^{-2i\mathcal{J}_{nm}\bar{t}} \sin^2(\phi_m) \right) i e^{-i\theta_n} \sin(\phi_n) \cos(\phi_n) e^{ih_n\bar{t}} K_{\bar{t}}(m, n) + H.c.. \quad (\text{C9})$$

Finally let us compute now the last correlation terms:  $\langle \hat{\tau}_m^{\alpha=x,y}(t) \hat{\tau}_n^{\alpha'=x,y}(t) \rangle$ , which can be written as

$$\hat{\tau}_m^\alpha(t) \hat{\tau}_n^{\alpha'}(t) = \sum_{b_m, b_n=0,1} \hat{X}_{m,n}^{(\alpha, b_m)(\alpha', b_n)} \quad (\text{C10})$$

The solution can be cast in the form

$$\hat{\tau}_m^\alpha(t) = \hat{C}_m^{\alpha,-} e^{i\hat{A}_m t} + \hat{C}_m^{\alpha,+} e^{-i\hat{A}_m t}, \quad (\text{C5})$$

where

$$\hat{C}_m^{\alpha,\pm} = \frac{\hat{\tau}_m^\alpha(0) \pm i\epsilon_{z\alpha\bar{\alpha}} \hat{\tau}_m^{\bar{\alpha}}(0)}{2}.$$

Given the above expressions, we will now explicitly show the expectation values for all local and two-point correlations. In order to compute the correlations we will extensively use the following identity

$$e^{i\hat{A}_m t} = e^{ih_m \mathbb{I} \bar{t}} e^{2i\mathcal{J}_{mn} \hat{\tau}_n^z \bar{t}} \left( \prod_{j \neq m, n} e^{2i\mathcal{J}_{mj} \hat{\tau}_j^z \bar{t}} \right) \quad (\text{C6})$$

with  $\bar{t} = -\frac{2}{\hbar} t$ .

**Local averages -** For the  $z$ -spin terms we have that

$$\langle \tau_m^z(t) \rangle = \langle \tau_m^z(0) \rangle = \underbrace{\cos^2(\phi_m) - \sin^2(\phi_m)}_{z_m}. \quad (\text{C7})$$

For the  $x$ -spin term we obtain

$$\langle \tau_m^x(t) \rangle = \sin(\phi_m) \cos(\phi_m) \left[ e^{-i\theta_m} e^{ih_m \bar{t}} K_{\bar{t}}(m, m) + H.c. \right]$$

where  $\bar{t} = -\frac{2}{\hbar} t$ , and

$$K_{\bar{t}}(m, n) = \prod_{j \neq m} \left( e^{2i\mathcal{J}_{nj}\bar{t}} \cos^2(\phi_j) + e^{-2i\mathcal{J}_{nj}\bar{t}} \sin^2(\phi_j) \right).$$

An analogous expression holds for the for the  $y$ -component.

**Two-point correlations:** For the  $zz$ -correlations we have

$$\langle \hat{\tau}_m^z(t) \hat{\tau}_n^z(t) \rangle = \langle \hat{\tau}_m^z(0) \hat{\tau}_n^z(0) \rangle = z_m z_n.$$

with

$$\begin{aligned} \hat{X}_{m,n}^{(\alpha,b_m)(\alpha',b_n)} &= \hat{C}_m^{\alpha,-b_m} e^{b_m i \hat{A}_m t} \hat{C}_n^{\alpha',-b_n} e^{b_n i \hat{A}_n t} \\ &= \underbrace{\hat{C}_m^{\alpha,-b_m} e^{i(b_m h_m \mathbb{I} + b_n 2 \mathcal{J}_{nm} \hat{\tau}_m^z) \bar{t}}}_{m \text{ site}} \underbrace{e^{i(b_n h_n \mathbb{I} + b_m 2 \mathcal{J}_{mn} \hat{\tau}_n^z) \bar{t}} \hat{C}_n^{\alpha',-b_n}}_{n \text{ site}} \underbrace{\left( \prod_{j \neq m,n} e^{2i(b_m \mathcal{J}_{mj} + b_n \mathcal{J}_{nj}) \hat{\tau}_j^z \bar{t}} \right)}_{\text{rest}}. \end{aligned} \quad (\text{C11})$$

The expectation value for  $\langle \hat{X}_{m,n}^{(\alpha,b_m)(\alpha',b_n)} \rangle$  is given by

$$\langle \hat{X}_{m,n}^{(\alpha,b_m)(\alpha',b_n)} \rangle = e^{i(b_m k_m + b_n k_n) \bar{t}} G_{\bar{t}}^{\alpha}(m, n, b_m, b_n) G_{\bar{t}}^{\alpha'}(n, m, -b_n, -b_m)^* F_{\bar{t}}(m, n, b_m, b_n) \quad (\text{C12})$$

where

$$\begin{aligned} F_{\bar{t}}(m, n, b_m, b_n) &\equiv \prod_{j \neq m,n} [ e^{2i(b_m \mathcal{J}_{mj} + b_n \mathcal{J}_{nj}) \bar{t}} \cos^2(\phi_j) \\ &\quad + e^{-2i(b_m \mathcal{J}_{mj} + b_n \mathcal{J}_{nj}) \bar{t}} \sin^2(\phi_j) ] \end{aligned}$$

and

$$\begin{aligned} G_{\bar{t}}^x(m, n, -1, b_n) &= e^{-b_n i 2 \mathcal{J}_{nm} \bar{t}} e^{i \theta_m} \sin(\phi_m) \cos(\phi_m) \\ G_{\bar{t}}^x(m, n, +1, b_n) &= e^{b_n i 2 \mathcal{J}_{nm} \bar{t}} e^{-i \theta_m} \sin(\phi_m) \cos(\phi_m) \\ G_{\bar{t}}^y(m, n, -1, b_n) &= -i \langle \hat{C}_m^{+,+} e^{i b_n 2 \mathcal{J}_{nm} \hat{\tau}_m^z \bar{t}} \rangle \\ G_{\bar{t}}^y(m, n, +1, b_n) &= i \langle \hat{C}_m^{-,-} e^{i b_n 2 \mathcal{J}_{nm} \hat{\tau}_m^z \bar{t}} \rangle. \end{aligned}$$

Using Eqs.(C10) and (C12),  $\langle \hat{\tau}_m^{\alpha=x,y}(t) \hat{\tau}_n^{\alpha'=x,y}(t) \rangle$  can be computed .

- 
- <sup>1</sup> D. Basko, I. Aleiner, and B. Altshuler, *Ann. Phys.* **321**, 1126 (2006).
  - <sup>2</sup> V. Oganesyan and D. Huse, *Phys. Rev. B* **75**, 155111 (2007).
  - <sup>3</sup> R. Nandkishore and D. A. Huse, *Annual Review of Condensed Matter Physics* **6**, 15 (2015).
  - <sup>4</sup> M. V. Berry, Semiclassical mechanics of regular and irregular motion, in *Les Houches, Session XXXVI, 1981 — Chaotic Behaviour of Deterministic Systems*, edited by R. S. G. Ioos, R. H. G. Helleman, pp. 174–271, North-Holland Publishing Company, 1983.
  - <sup>5</sup> V. I. Arnol'd, *Mathematical Methods of Classical Mechanics* (Springer, 1989).
  - <sup>6</sup> A. Polkovnikov, K. Sengupta, A. Silva, and M. Vengalattore, *Rev. Mod. Phys.* **83**, 863 (2011).
  - <sup>7</sup> Maksym Serbyn, Z. Papic, and Dmitry A. Abanin, *Phys. Rev. Lett.* **111**, 127201 (2013).
  - <sup>8</sup> V. Ros, M. Mueller, and A. Scardicchio, *Nuclear Physics B* **891**, 420 (2015).
  - <sup>9</sup> A. Chandran, I. H. Kim, G. Vidal, and D. A. Abanin, *Phys. Rev. B* **91**, 085425 (2015).
  - <sup>10</sup> J. Z. Imbrie, *Jour. Stat. Phys* **163**, 998 (2016).
  - <sup>11</sup> P. Calabrese, F. H. L. Essler, and G. Mussardo (editors), *Quantum Integrability in Out of Equilibrium Systems*, special issues of *J. Stat. Mech.* (IOPScience, 2016), url: <http://stacks.iop.org/1742-5468/2016/i=6/a=064001>.
  - <sup>12</sup> M. Schiulaz, A. Silva, and M. Müller, *Phys. Rev. B* **91**, 184202 (2015).
  - <sup>13</sup> M. Pino, B. L. Altshuler, and L. B. Ioffe, arXiv:1501.03853 (2015).
  - <sup>14</sup> P. Anderson, *Phys. Rev.* **109**, 1492 (1958).
  - <sup>15</sup> E. Abrahams (editor) *50 years of Anderson localization* (World Scientific, 2010).
  - <sup>16</sup> A. Pal and D. A. Huse, *Phys. Rev. B* **82**, 174411 (2010).
  - <sup>17</sup> D. J. Luitz, N. Laflorencie, and F. Alet, *Phys. Rev. B* **93**, 060201 (2016).
  - <sup>18</sup> M. Žnidarič, A. Scardicchio, and V. K. Varma, *Phys. Rev. Lett.* **117**, 040601 (2016).
  - <sup>19</sup> V. Kerala Varma, A. Leroose, F. Pietracaprina, J. Goold, and A. Scardicchio, arXiv:1511.09144 (2015).
  - <sup>20</sup> D. A. Huse, R. Nandkishore, and V. Oganesyan, *Phys. Rev. B* **90**, 174202 (2014).
  - <sup>21</sup> A. Chandran, I. H. Kim, G. Vidal, and D. A. Abanin, *Phys. Rev. B* **91**, 085425 (2015).
  - <sup>22</sup> M. Žnidarič, T. Prosen, and P. Prelovšek, *Phys. Rev. B* **77**, 64426 (2008).
  - <sup>23</sup> J. H. Bardarson, F. Pollmann, and J. E. Moore, *Phys. Rev. Lett.* **109**, 017202 (2012).
  - <sup>24</sup> Maksym Serbyn, Z. Papic, and Dmitry A. Abanin, *Phys. Rev. Lett.* **110**, 260601 (2013).
  - <sup>25</sup> A. De Luca and A. Scardicchio, *Europhys. Lett.* **101**, 37003 (2013).
  - <sup>26</sup> C. Monthus, *J. Stat. Mech.*, P033101 (2016).
  - <sup>27</sup> E. Canovi, D. Rossini, R. Fazio, G. E. Santoro, and A. Silva, *Phys. Rev. B* **83**, 094431 (2011).
  - <sup>28</sup> Maksym Serbyn, Z. Papic, and D. A. Abanin, *Phys. Rev. B* **90**, 174302 (2014).
  - <sup>29</sup> R. Berkovits, *Phys. Rev. Lett.* **108**, 176803 (2012).
  - <sup>30</sup> B. Bauer, and C. Nayak, *J. Stat. Mech.*, P09005 (2013).
  - <sup>31</sup> A. Pal and D. A. Huse, *Phys. Rev. B* **82**, 174411 (2010).
  - <sup>32</sup> D. A. Huse, R. Nandkishore, V. Oganesyan, A. Pal, and S. Sondhi, *Phys. Rev. B* **88**, 014206 (2013).
  - <sup>33</sup> E. Altman and R. Vosk, *Annual Review of Condensed Matter Physics* **6**, 383 (2015).

- <sup>34</sup> M. Serbyn, M. Knap, S. Gopalakrishnan, Z. Papić, N.Y. Yao, C.R. Laumann, D.A. Abanin, M.D. Lukin, and E.A. Demler, *Phys. Rev. Lett.* **113**, 147204 (2014).
- <sup>35</sup> R. Vasseur, S. A. Parameswaran, and J. E. Moore *Phys. Rev. B* **91**, 140202 (2015).
- <sup>36</sup> M. Schreiber *et al.*, *Science* **349**, 842 (2015).
- <sup>37</sup> P. Bordia, H. Lüschen, U. Schneider, M. Knap, and I. Bloch, *arXiv:1607.07868* (2016).
- <sup>38</sup> J. Smith, A. Lee, P. Richerme, B. Neyenhuis, P. W. Hess, P. Hauke, M. Heyl, D. A. Huse, and C. Monroe *Nat. Phys.*, doi:10.1038/nphys3783 (2016).
- <sup>39</sup> T. Fukuhara *et al.*, S. Hild, J. Zeiher, P. Schauß, I. Bloch, M. Endres, and C. Gross *Phys. Rev. Lett.* **115**, 035302 (2015).
- <sup>40</sup> P. Jurcevic *et al.*, *Nature* **511**, 202 (2014).
- <sup>41</sup> G. De Chiara, S. Montangero, P. Calabrese, and R. Fazio, *J. Stat. Mech.*, 0603:L03001 (2006), cond-mat/0512586.
- <sup>42</sup> D.-L. Deng, X. Li, J. H. Pixley, Y.-L. Wu, and S. D. Sarma, *arXiv:1607.08611* (2016).
- <sup>43</sup> A. M. Kaufman *et al.*, *arXiv:1603.04409* (2016).
- <sup>44</sup> S. Aubry and G. André, Analyticity breaking and anderson localization in incommensurate lattices, in *Group theoretical methods in physics (Proc. Eighth Internat. Colloq., Kiryat Anavim, 1979)*, , Ann. Israel Phys. Soc. Vol. 3, pp. 133–164, Hilger, Bristol, 1980.
- <sup>45</sup> A. B. Kuklov and B. V. Svistunov, *Phys. Rev. Lett.* **90**, 100401 (2003).
- <sup>46</sup> L.-M. Duan, E. Demler, and M. Lukin, *Phys. Rev. Lett.* **91**, 090402 (2003).
- <sup>47</sup> V. Mastropietro, *Phys. Rev. Lett.* **115**, 180401 (2015).
- <sup>48</sup> G. Roati, C. D’Errico, L. Fallani, M. Fattori, C. Fort, M. Zaccanti, G. Modugno, M. Modugno, and M. Inguscio, *Nature* **453**, 895 (2008).
- <sup>49</sup> W. K. Wootters, *Phys. Rev. Lett.* **80**, 2245 (1998).
- <sup>50</sup> L. Amico, R. Fazio, A. Osterloh, and V. Vedral, *Rev. Mod. Phys.* **80**, 517 (2008).
- <sup>51</sup> V. Coffman, J. Kundu, and W. K. Wootters, *Phys. Rev. A* **61**, 052306 (2000).
- <sup>52</sup> T. Osborne and F. Verstraete, *Phys. Rev. Lett.* **96**, 220503 (2006).
- <sup>53</sup> A. J. Daley, C. Kollath, U. Schollwöck, and G. Vidal, *J. Stat. Mech.*, P04005 (2004).
- <sup>54</sup> U. Schollwöck, *Ann. Phys.* **326**, 96 (2011).
- <sup>55</sup> S. Bera and A. Lakshminarayan, *Phys. Rev. B* **93**, 134204 (2016).
- <sup>56</sup> The distribution of  $\mathcal{J}_{jl}$  for a local MBL model has long tails, as found in<sup>8,64</sup>. However, we find that this does not qualitatively change our results.
- <sup>57</sup> L. Mazza, D. Rossini, R. Fazio, and M. Endres, *New J. Phys.* **17**, 013015 (2015).
- <sup>58</sup> F. Buccheri, A. De Luca, and A. Scardicchio, *Phys. Rev. B* **84**, 094203 (2011).
- <sup>59</sup> D. J. Luitz and Y. B. Lev, *arXiv:1607.01012* (2016).
- <sup>60</sup> V. Oganesyan and D. A. Huse, *Phys. Rev. A* **75**, 155111 (2007).
- <sup>61</sup> F. Haake, *Quantum Signatures of Chaos* (2<sup>nd</sup> ed) (Springer, 2001).
- <sup>62</sup> M. V. Berry and M. Tabor, *Proc. Roy. Soc. A* **349**, 101 (1976).
- <sup>63</sup> D. Poilblanc, T. Ziman, J. Bellisard, F. Mila, and G. Montambaux, *Europhys. Lett.* **22**, 537 (1993).
- <sup>64</sup> D. Pekker, B. Tian, X. Yu, B. Clark, and V. Oganesyan, Identifying the local conserved quantities in many-body-localized matter, in *APS Division of Atomic, Molecular and Optical Physics Meeting Abstracts* Vol. 1, p. 6001P, 2015.
- <sup>65</sup> Steve Campbell, Matthew J. M. Power, and Gabriele De Chiara, *arXiv:1608.08897* (2016).
- <sup>66</sup> Giuseppe De Tomasi, Soumya Bera, Jens H. Bardarson, and Frank Pollmann, *arXiv:1608.07183* (2016).